ChemPubSoc Europe

DOI: 10.1002/ejic.201501255

EurJIC European Journal of Inorganic Chemistry

Full Paper

Chain Compounds

Preparation, First Structure Analysis, and Magnetism of the Long-Known Nickel Benzoate Trihydrate – A Linear Ni···Ni···Ni Polymer and Its Parallels with the Active Site of Urease

Anna Vráblová,[a] Larry R. Falvello,[b] Javier Campo,[c] Jozef Miklovič,[d] Roman Boča,[d] Juraj Černák*[a] and Milagros Tomás[e]

Abstract: Nickel benzoate trihydrate (**1**) has been prepared in single-crystalline form by the reaction of nickel carbonate with benzoic acid in boiling aqueous solution. Its crystal structure comprises positively charged $[Ni(Bz)(H_2O)_2]_n^{n+}$ chains, benzoate anions, and one independent water molecule of solvation. The hexacoordinate Ni^{II} centers in the chains are triply bridged by one *syn-syn* carboxylato and two aqua bridges, and adjacent chains are linked by O–H···O hydrogen bonds [O···O distances are in the range 2.647(3)–2.684(3) Å] through solvate water molecules and benzoate anions. Thermal analysis revealed that **1** is stable up to 100 °C; further heating led to full dehydration accompanied by an additional decomposition reaction, as characterized by IR analysis of the intermediates. The geometrical features of the Ni centers have been compared with similar features at the active sites of urease. The effective magnetic moment per formula unit μ_{eff} has a value of 3.17μ_B at room temperature and upon cooling reaches a maximum value of 12.39μ_B at T = 4.6 K, which indicates ferromagnetic coupling between the nearest Ni^{II} atoms [3.0671(1) Å] within the chains; at lower temperatures this is counteracted by zero-field splitting.

Introduction

If chemical simplicity could be conflated reliably with ease of preparation and characterization, then various forms of nickel benzoate, the trihydrate of which is the subject of this report, would have been characterized many decades ago. The trihydrate has long been known, its preparation reported by Ephraim and Pfister[1] in 1925 and by Pfeiffer and Müllenheim[2] in 1933. From that time several partial studies of different forms of nickel benzoate (trihydrate, tetrahydrate, anhydrous) have been reported.[3–5] More recently, the crystal structure of the dinuclear "paddle-wheel"-type complex $[Ni_2(\mu_2\text{-}Bz)_4(HBz)_2]$, formed fortuitously under solvothermal conditions beginning with nickel(II) nitrate, sodium benzoate, and 2,2′-bipyridine, has been reported.[6] However, a structure analysis of the title trihydrate by diffraction methods, the present-day sine qua non standard for characterizing new coordination compounds, has remained elusive.

As one of the simpler and more easily handled carboxylates, benzoate has been used in studies of more complex systems in which carboxylates are common, such as MOFs[7] and magnetic solids.[8] The ubiquity of carboxylates in natural compounds is well known, including in enzymes[9] in which, inter alia, they participate at the active sites of biocatalytic processes.

The different manners in which a carboxylate function such as that of benzoate can coordinate metal centers, namely as a terminal, chelating, or bridging ligand, permit a wide variability in the processes and structures in which this group is involved. As a bridge, carboxylate participates in discrete molecules and extended nets, and possesses a special capacity for drawing metal centers closer together than do, for example, cyanide or azide bridges. This property propitiates magnetic interactions and can activate metal centers for catalytic applications.

Among the metals that have been studied in carboxylate complexes, nickel(II), when six-coordinate, that is, in an octahedral coordination or in a distorted shape derived from the octahedron, is expected to be paramagnetic with S = 1. Nickel also appears at the active sites of numerous enzymes,[10] including urease, in which two nickel atoms bridged by one carboxylate and one water molecule are present at the active sites;[11] compounds with two nickel atoms bridged by two carboxylate

[a] *Department of Inorganic Chemistry, P. J. Šafárik University in Košice, Moyzesova 11, 04154 Košice, Slovakia*
E-mail: juraj.cernak@upjs.sk
www.upjs.sk
[b] *Departamento de Química Inorgánica, Instituto de Ciencia de Materiales de Aragón (ICMA), University of Zaragoza-CSIC, Pedro Cerbuna 12, 50009 Zaragoza, Spain*
[c] *Departamento de Física de la Materia Condensada, University of Zaragoza-CSIC, Pedro Cerbuna 12, 50009 Zaragoza, Spain*
[d] *Department of Chemistry, FPV, University of SS Cyril and Methodius, 91701 Trnava, Slovakia*
[e] *Departamento de Química Inorgánica, Instituto de Síntesis Química y Catálisis Homogénea (ISQCH), University of Zaragoza-CSIC, Pedro Cerbuna 12, 50009 Zaragoza, Spain*

Supporting information and ORCID(s) from the author(s) for this article are available on the WWW under http://dx.doi.org/10.1002/ejic.201501255.

groups and one water molecule have been used as model systems for understanding the workings of urease.[12,13]

Ni^{II} complexes with one-dimensional (1D) polymeric structures and with $S = 1$ have been the subject of many experimental and theoretical studies associated with magnetic phenomena.[14–19] The synthesis of 1D Ni^{II} coordination polymers is usually mediated by suitable bridging ligands linking Ni^{II} central atoms, for example, pyrazine (pyr) in $\{[Ni(pyr)(H_2O)_4](NO_3)_2 \cdot 2H_2O\}_n$,[20] bromide anions in $[Ni(Br)_2(tz)_2]_n$ (tz = 1,3-thiazole),[21] or azido anions in $[Ni(3,5\text{-dmpy})_2(N_3)_2]_n$ (3,5-dmpy = 3,5-dimethylpyridine).[22] Using the complex anion $[Ni(CN)_4]^{2-}$ as a bridging unit, we have previously synthesized several chain-like structures, for example, $[Ni(en)_2Ni(CN)_4]$[23] and $[Ni(dien)(mea)Ni(CN)_4]$ (dien = diethylenetriamine, mea = 2-aminoethanol).[24] The disadvantage of these cyanide complexes as regards their magnetism is the large distance between the paramagnetic Ni^{II} atoms (approximately 10 Å), which results in very weak intrachain exchange interactions. Recently, in our quest for 1D Ni^{II} systems with shorter separations between Ni^{II} centers, we prepared a microcrystalline sample of the Haldane gap system $[Ni(bpy)(ox)]_n$ (bpy = 2,2-bipyridine, ox = oxalate) in which the Ni^{II} atoms are bridged in bis-chelating fashion by oxalate.[25]

As a continuation of our studies on 1D Ni^{II} coordination polymers, we report herein the preparation of $\{[Ni(Bz)(H_2O)_2] \cdot Bz \cdot H_2O\}_n$ (**1**; HBz = benzoic acid) in single-crystal form, its magnetism, and its crystal structure analysis, which reveals a geometrically linear Ni···Ni···Ni polymeric structure with a small Ni···Ni separation of 3.0671(1) Å. Within the chain, pairs of nickel centers are triply bridged by a carboxylate and two water molecules. The triple bridge presents interesting similarities to the active site of urease, including its hydrogen-bonding interactions with uncoordinated water molecules.

Results and Discussion

We have prepared complex **1** in single-crystal form by the reaction of nickel(II) carbonate with a slight excess of benzoic acid in boiling water. The product as isolated contained benzoic acid as an impurity, but this could be removed by rinsing with ethanol. The purity and identity of the product were checked by chemical analysis. In addition, the powder X-ray diffraction pattern was recorded to confirm that the phase identity of the bulk sample was the same phase characterized in the single-crystal X-ray study (see Figure S1 in the Supporting Information).

The IR spectrum of **1** is rich in content (Figure 1), but some characteristic absorption bands can be identified. A broad absorption band of medium intensity centered at around 2965 cm^{-1} can be attributed to ν(OH) stretching vibrations of the solvate water molecules and aqua ligands. The observed shift of this band to lower wave numbers can be explained by the participation of the water molecules in medium-to-strong hydrogen bonds (HBs; see below). This band has a shoulder, a very weak absorption at 3054 cm^{-1} attributable to a C_{ar}–H stretching vibration, as indicated by Nakamoto;[26] in the IR spectrum of benzoic acid this vibration is positioned at 3070 cm^{-1}. The presence of the aromatic rings is also corroborated by the sharp absorption band observed at 1593 cm^{-1}, which can be attributed to the C_{ar}–C_{ar} in-ring stretching vibration. The most characteristic absorption bands are the ones due to the asymmetric (1547, 1494 cm^{-1}) and symmetric (1424, 1384 cm^{-1}) stretching modes of the COO^- groups. We note that Pavkovic reported similar values of 1553, 1500, 1440, and 1392 cm^{-1} for the trihydrate.[3]

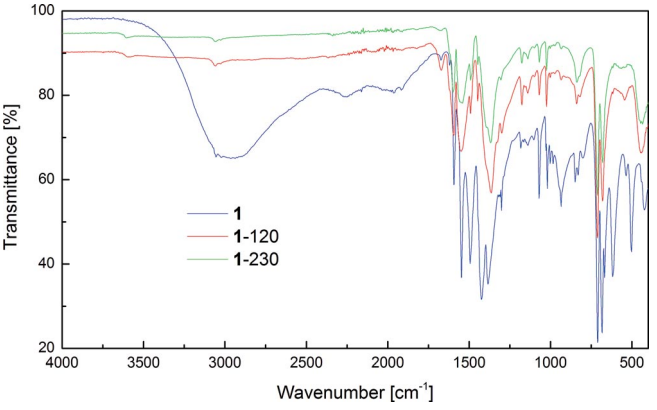

Figure 1. Comparison of the IR spectra of samples **1** (blue trace), **1**-120 (sample heated at 120 °C, red), and **1**-230 (sample heated at 230 °C, green).

To study the thermal stability as well as the dehydration of **1**, its thermal curves were recorded (Figure 2). As can be seen from the TG curve in Figure 2, complex **1** is stable up to 100 °C. Over the broad temperature range 100–330 °C, a total weight loss of 21.3 % occurs, which can be seen (Figure 2) to comprise at least two successive processes. The first occurs in the temperature range 100–160 °C and corresponds to a rapid endothermic weight loss of 14.0 %, and the second part, over the larger temperature range of 160–330 °C, manifests itself by a much slower weight loss amounting in the end to 7.3 %. We note that the calculated weight loss for the total dehydration of **1** is 15.2 %, which suggests that, besides dehydration, another reaction(s) is taking place. To obtain more insight into the observed processes, samples of **1** were heated in an oven at 120 and 230 °C for 30 min (samples **1**-120 and **1**-230, respectively). The IR spectrum of **1**-120 (Figure 1) indicates the absence of water molecules in the sample; in addition, substantial changes in the shape and positions of the absorption bands of the asymmetric and symmetric modes of COO^- can be observed. The IR spectrum of **1**-230 is similar to that of **1**-120 with a decrease in the intensities of all bands. It is interesting to note the presence of a weak absorption near 3600 cm^{-1}, which may correspond to an O–H stretching vibration in the absence of hydrogen bonding. These results suggest that the thermal decomposition of **1** starts with dehydration, as was reported for the similar tetrahydrate[27] and the analogous hydrate of the 2-chloro-4-nitrobenzoate of Ni^{II}.[28] As to the further, much slower decomposition process, several scenarios are possible; among these is partial decarboxylation. We note that it has been reported that benzoic acid can be transformed into phenol by oxidative decarboxylation[29a] (the Dow Phenol Process) in the presence of water over NiO[29b] or by using copper benzoate as catalyst.[30] The calculated weight loss for such a combination of processes

($3 \times H_2O$ and $1 \times CO_2$ with one oxygen atom coming from the atmosphere) is 23.1 %, which is comparable to the observed weight loss of 21.3 %.

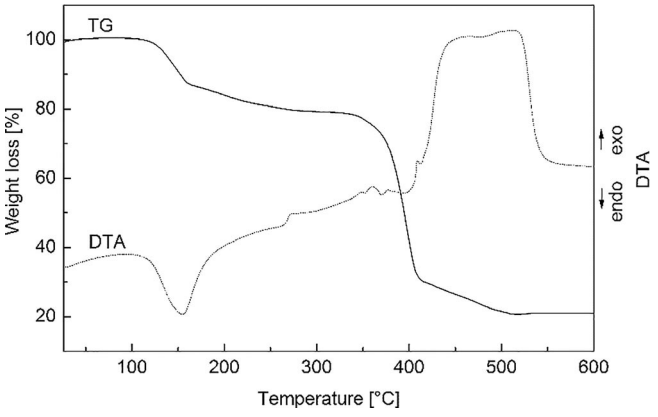

Figure 2. TGA curves of **1**.

Further heating of **1** in the temperature range 320–530 °C leads to a strong exothermic decomposition of its organic component. The residual mass of 20.7 % is in good agreement with the calculated residual mass for NiO (21.0 %); the formation of NiO was also reported in the case of the thermal decomposition of the anhydrous Ni^{II} benzoate in air.[31]

As expected, anhydrous $Ni(Bz)_2$ displayed enhanced thermal stability (230 °C) and upon the observed mass loss the formation of NiO as a solid residue was reported.[4] On the other hand, the tetrahydrate $Ni(Bz)_2 \cdot 4H_2O$ is stable only up to 100 °C (as was observed for **1**) and the formation of metallic nickel was reported at the end of the thermal decomposition.[5]

The crystal structure of **1** is composed of positively charged $[Ni(Bz)(H_2O)_2]_n^{n+}$ chains, benzoate anions, and solvate water molecules (Figure 3 and Figure 4). The chains are built up of triply bridged pairs of Ni^{II} atoms; two bridges are formed by μ_2-aqua ligands and the third by a *syn-syn*-benzoate ligand. Although the Ni···Ni···Ni chains are strictly linear, running parallel to the crystallographic *a* axis, the axial coordination directions at the Ni^{II} atoms, that is, the Ni1···O1 and symmetry related bonds, are tilted by 12.34(7)° with respect to the *b* axis.

The Ni^{II} center (–1 site) is hexacoordinate (donor set O_2O_4) in the form of a compressed bipyramid (Figure 3). The axial Ni1–O1 bond lengths [1.9654(18) Å; 2 ×] are shorter than those in the equatorial plane, 2.0979(19) and 2.1270(18) Å (Table 1). The observed compression of the octahedron can be expressed by the ratio $\kappa = (Ni–O)_{ax}/\langle(Ni–O)_{eq}\rangle = 0.93$. A similar compression of the octahedral coordination of Ni^{II} was found in $[Ni(H_2O)_6][Zn(H_2O)_2(phen)_2]_2 \cdot 2btc \cdot H_2O$ (phen = 1,10-phenanthroline; btc = 1,3,5-benzenetricarboxylate)[32] with the value $\kappa = 0.95$; a similar value of $\kappa = 0.94$ was found in $\{[Ni(cbab)(H_2O)_2] \cdot H_2O\}_n$ [cbab = 4-(4-carboxybenzoylamino)-benzoate] bearing the μ_2-bridging aqua ligand.[27] The Ni–$O(H_2)$–Ni angle in **1** is 93.09(7)°.

Reports of Ni compounds in which the Ni atoms are triply bridged by a carboxylate and two water molecules are scarce, comprising just a single family of hexanickel(II) complexes with Ni···Ni distances between 3.105 and 3.111 Å.[33] The triple

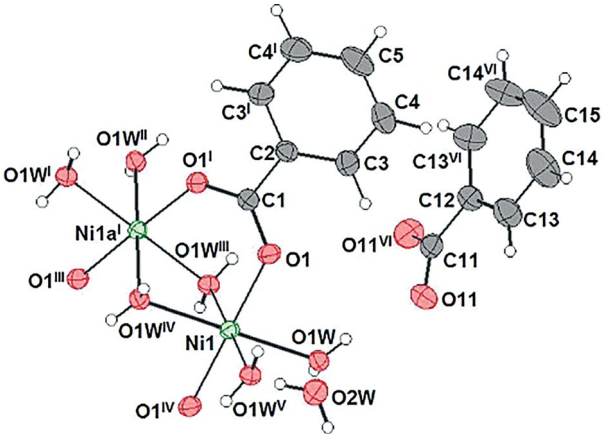

Figure 3. One segment of the structure of **1** with the atom numbering scheme. Displacement ellipsoids are drawn at the 50 % probability level. Symmetry codes: i: 1.5 – *x*, *y*, 1 – *z*; ii: 1 + *x*, *y*, *z*; iii: 0.5 + *x*, 1 – *y*, *z*; iv: 1 – *x*, 1 – *y*, 1 – *z*; v: 0.5 – *x*, *y*, 1 – *z*; vi: 0.5 – *x*, *y*, –*z*.

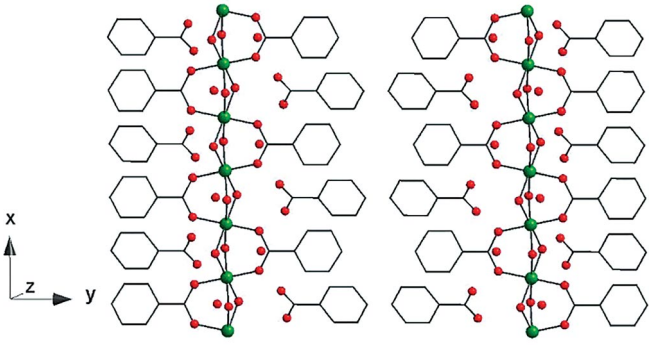

Figure 4. Polymeric structure of **1**.

Table 1. Selected bond lengths [Å] and angles [°] for **1**.

Ni1–O1	1.9654(18)	C1–O1	1.270(2)
Ni1–O1W	2.1270(18)	C11–O11	1.261(3)
Ni1–O1W^v	2.0979(19)		
O1–Ni1–O1W	87.16(7)	Ni1–O1W–Ni1^v	93.09(7)
O1–Ni1–O1W^v	90.61(8)	O1–C1–O1^v	125.3(3)
O1W–Ni1–O1W^v	83.39(8)	O11–C11–O11^{vi}	124.2(4)

Symmetry codes: v: 0.5 – *x*, *y*, 1 – *z*; vi: 0.5 – *x*, *y*, –*z*.

bridge in compound **1** coincides with a Ni···Ni separation of 3.0671(1) Å, and the extended chain has Ni···Ni···Ni angles of 180°. Very few linear Ni^{II}···Ni^{II}···Ni^{II} 1D polymers, that is, with angles of 170–180° and distances between Ni atoms of less than 4 Å, have been reported in metal–organic crystals. In the known examples, the bridges are mainly chlorine or bromine atoms, although some structures with S (benzenethiolato: Ni···Ni distance = 3.173 Å)[34] or pyrazolate bridges (Ni···Ni distance = 3.471 Å)[35] have been reported. The Ni···Ni distances in the 1D polymers with halogen bridges depend on the number of bridges (two or three) and the nature of the halogen, the shortest being those with triple chlorine bridges (for instance, with an Ni···Ni distance of 3.063 or 3.060 Å)[36] with Ni···Ni separations similar to those in compound **1**.

Binuclear nickel compounds with carboxylate and water bridges are of interest as models for the active centers of en-

zymes.[10,11] Although the number of nickel compounds with a carboxylate and two aqua bridges, as in compound **1**, is very small, nickel compounds with one aqua and two carboxylate bridges are more common. Some of these compounds have been used as models for the active site of the enzyme urease,[12] because the active site contains two nickel atoms bridged by a single carboxylate and a single water molecule with a terminal water molecule at each of the nickel centers (Figure 5a). It is not clear whether all of the sites identified as water in urease are indeed water or whether some are hydroxide. Neither is it clear yet how the urease catalyzes the hydrolysis of urea into two ammonia molecules and carbonic acid; but the common first step in all of the proposed mechanisms is the binding of urea to one of the nickel atoms, displacing the terminal water. In Figure 5 we can see that a similar result would be obtained if urea were to coordinate to one of the nickel centers in compound **1**, breaking one of the water bridges. That would leave one terminal and one bridging water in addition to the newly bound terminal urea. Therefore, compound **1** is of potential interest as a model for studying the mechanism of urease activity, or as a precursor for other, related compounds.

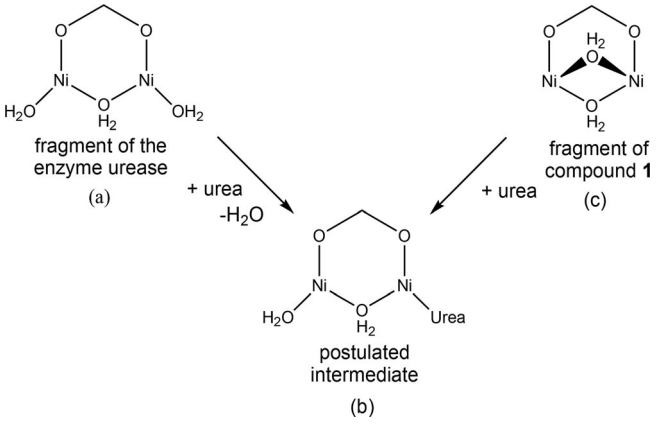

Figure 5. First step in the previously proposed mechanism of urease activity [(a) → (b)] and the hypothetical parallel reactivity of compound **1** [(c) → (b)].

The water molecules and carboxylate oxygen atoms in **1** are involved in O–H···O hydrogen bonds of considerable strength, as indicated by the short O···O distances in the range 2.647(3)–2.684(3) Å and O–H···O angles close to linearity (Table 2, Figure 6).

Table 2. Hydrogen bonds [Å, °] for **1**.

D–H···A	D–H [Å]	H···A [Å]	D···A [Å]	D–H···A [°]
O1W–H1A···O11	0.76(3)	1.90(3)	2.647(3)	169(3)
O1W–H1B···O2W	0.81(3)	1.88(3)	2.684(3)	172(3)
O2W–H2A···O11^{vii}	0.82(3)	1.86(3)	2.679(2)	172(3)

Symmetry codes: vii: –*x*, 1 – *y*, –*z*

Some of the hydrogen bonds are formed between the bridging water molecules and the free benzoate groups, O1W–H1A···O11, which further polarizes the water O···H bond, favoring a putative deprotonation to give HO^- groups in compound **1**, in a further possible analogy to the active site of urease.

One consequence of the formation of strong hydrogen bonds is the shape of the observed ν(OH) absorption band in the IR spectrum (all hydrogen atoms are involved in hydrogen bonding) as well as the observed shift of its position to 2965 cm^{-1}. The hydrogen-bonding system connects covalent chains into supramolecular layers perpendicular to the *b* axis (Figure 6). The active site of urease also contains one external water molecule that forms strong hydrogen bonds with the coordinated water molecules.

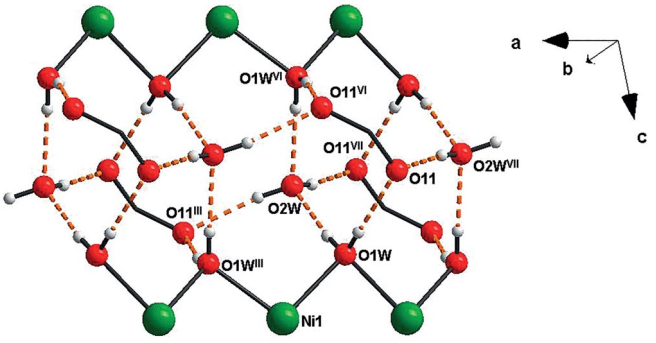

Figure 6. Hydrogen-bonding scheme in **1**. Symmtery codes: iii: 0.5 + *x*, 1 – *y*, *z*; vi: 0.5 – *x*, *y*, –*z*; vii: –*x*, 1 – *y*, –*z*.

For both benzoate fragments the delocalization of π electrons between the aromatic ring and the carboxylate group is hindered, as the dihedral angles between the ring and COO^- are 15.17(9)° (benzoate containing C1) and 14.4(3)° (C11). The twist is likely a result of weak C–H···π interactions between neighboring phenyl rings (Figure 7, Table 3). Evidence of π delocalization was observed in the structure of $[Ni_2(\mu_2\text{-}Bz)_4(HBz)_2]$, in which the dihedral angle between the aromatic ring and the plane defined by the carboxylate group has values of 1.2, 12.7, and 7.7° for the three independent benzoato ligands.[6]

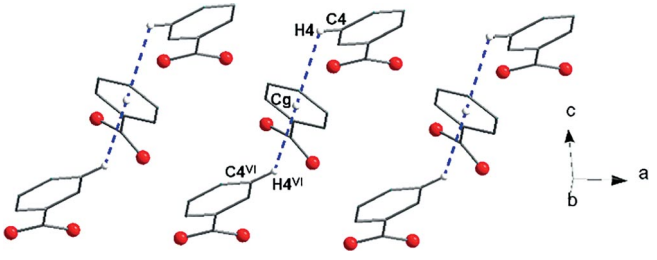

Figure 7. Weak C–H···π interactions between the phenyl rings in the crystal structure of **1**. Symmetry code: vi: 0.5 – *x*, *y*, –*z*.

Table 3. Possible weak hydrogen-bonding interactions for **1**.

C–H···Cg	C–H [Å]	H···Cg [Å]	C···Cg [Å]	C–H···Cg [°]
C4–H4···Cg2^{ii}	0.96(4)	2.93(3)	3.458(4)	116(3)

Symmetry code: ii: 1 + *x*, *y*, *z*

The structure of compound **1** is similar to that of $[Cu(H_2O)_2(Bz)]\cdot HBz\cdot H_2O$;[37] however, in **1**, the bridging water molecules are essentially symmetrically bonded to the nickel atoms [2.0979(19) and 2.1270(18) Å, O···Ni···O angle 83.39(8)°], whereas they are quite different in the copper compound (1.972 and 2.504 Å, angle 88.6°) due to the Jahn–Teller effect; this is the origin of the large difference in the unit-cell β angles for the two structures [95.331(3)° in compound **1** and 90.0° in

the copper analogue]. This is also the origin of the differences in their X-ray powder patterns, as noted by Pavkovic.[3]

The evolution of the magnetic properties of **1** (molar magnetic susceptibility, effective magnetic moment, magnetization per formula unit) is shown in Figure 8. The effective magnetic moment μ_{eff} is 3.17μ_B at room temperature, in accord with the presence of Ni^{II} ($S = 1$) centers. Upon lowering the temperature, the effective magnetic moment increases slowly at first, and then rapidly below 15 K, reaching a maximum of 12.39μ_B at $T = 4.6$ K. This is a fingerprint of the ferromagnetic exchange interaction ($J > 0$). The decrease in μ_{eff} at lower temperatures is due to single-ion anisotropy, expressed in terms of the zero-field splitting parameter D.

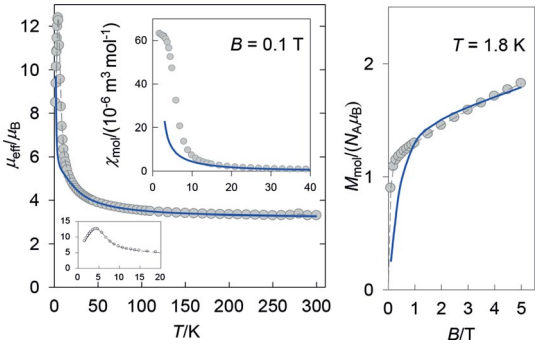

Figure 8. Magnetic functions for **1**: Left: Effective magnetic moment with detail (inset upper right) of the low-temperature range. Inset lower left: molar magnetic susceptibility. Right: Magnetization per formula unit. Solid lines represent the fitting.

When fitting the magnetic data it must be remembered that analytical formulae for the magnetic susceptibility in the case of $J > 0$ countermanded by D do not exist. The usual device for dealing with such a case is a finite ring approximation with the spin Hamiltonian given by Equation (1).

$$\hat{H}_\alpha = -\sum_{A<B}^{N} J(\vec{S}_A \cdot \vec{S}_B) + \sum_{A}^{N} D(\hat{S}_{A,z}^2 - \hat{S}_A^2/3) + \sum_{A}^{N} \mu_B B g \hat{S}_{A,\alpha} \quad (1)$$

in which the first summation is restricted to the nearest neighbors for the directions $\alpha = x, z$.

For $N = 4$, the fitting procedure converges to the following set of magnetic parameters: $J/hc = +12.1$ cm^{-1}, $g = 2.29$, $D/hc = +9.6$ cm^{-1}. The fit is very good for the higher-temperature tail of the magnetic susceptibility, thereby confirming that the Curie–Weiss law holds true in this region. Also, the molar magnetization is well reproduced for higher fields, which confirms the value (and also the sign) of the D parameter. However, the low-temperature region of the magnetic susceptibility and the low magnetic field of the magnetization are not reproduced well, which indicates that the magnetic interactions are more complex than the simple model of a finite ring. Note that the distance between the two neighboring Ni^{II} atoms within the chain is much shorter [3.0671(1) Å] than the shortest distance between the Ni^{II} atoms in neighboring chains [6.9793(2) Å] such that a putative interchain interaction would be weak.

Based on the Ni–O bond lengths (Table 1), the structural parameter D_{str} was calculated to be negative[38] ($D_{str} = -0.147$), in line with the presence of a compressed octahedron in **1**. Thus, one could expect that the zero-field splitting parameter D is negative. [D_{str} is calculated as $\Delta_z - (\Delta_y + \Delta_x)/2$, in which $\Delta_i = d_i - \langle d_i \rangle$, with the average $\langle d_i \rangle$ taken over all three ligand pairs.] Nevertheless, the quality of the fit with $D < 0$ is much worse than with $D > 0$.

Ferromagnetic interactions between Ni^{II} centers are not as common as their antiferromagnetic counterparts; examples of ferromagnetically coupled Ni^{II} atoms within chain-like arrangements have been reported, for example, in chiral [Ni(L/D-mand)(4-MePy)$_3$]$_n$•n(ClO_4) (Hmand = mandelic acid, 4-MePy = 4-methylpyridine)[32] and [Ni(1-tza)$_2$]$_n$ (1-Htza = tetrazole-1-acetic acid).[39]

Conclusions

The successful preparation and crystallization of nickel benzoate trihydrate, with formula $Ni(BzO)_2(H_2O)_3$, has permitted a thorough characterization of this substance, including of its crystal structure, some 90 years after its solubility properties were first reported by Ephraim and Pfister.[1] The 1D polymer described by the structure analysis, with a rigorously linear Ni···Ni···Ni chain, short intermetal distances, and axially compressed octahedral coordination at the Ni centers, correlates well with its magnetic properties, which reveal ferromagnetic intrachain coupling between the metal atoms and zero-field splitting, possibly alongside interchain antiferromagnetic interactions, which takes precedence below $T = 4.6$ K. In the crystal, with the Ni···Ni···Ni chain parallel to the a axis, supramolecular aggregation mediated by hydrogen bonds extends the structure along the ac plane, and C···H···π interactions add a third dimension by extending along [101].

Experimental Section

CHN analyses were performed with a Perkin–Elmer 2400 Series II CHNS/O analyzer. IR spectra were recorded with a Perkin–Elmer Spectrum 100 CsI DTGS FTIR spectrometer with a UATR 1 bounce-KRS-5 in the range 4000–300 cm^{-1} (UATR = universal attenuated total reflectance accessory; KRS-5 = thallium bromoiodide). The X-ray powder diffraction pattern of **1** (see Figure S1 in the Supporting Information) was recorded with a RIGAKU D-Max/2500 diffractometer with a rotating anode and RINT2000 vertical goniometer in the 2θ range 2.5–40° using Cu-$K_{\alpha 1}$ radiation ($\lambda = 1.5406$ Å) and a step size of 0.03°; the model powder diffraction pattern was calculated by using the Mercury program.[40] TG and DTG curves were recorded with a Netzch STA 409 PC/PG instrument under the following conditions: sample weight = 36.906 mg, heating rate = 10 K min^{-1}, dynamic artificial air atmosphere, temperature range 300–1174 K, aluminum oxide crucible.

Compound 1

A mixture of solid $NiCO_3$ (1.0 g; 7.7 mmol) and solid benzoic acid (2.0 g, 16.2 mmol) was slowly dissolved in water (250 mL) under heating and stirring to yield a green solution. Slow boiling was continued until cessation of gas liberation (approx. 45 min; the gas is likely CO_2). The loss of water was continuously compensated by the addition of boiling water. The hot solution was filtered and the filtrate was left aside for crystallization at room temperature. Within

a few days light-green crystals separated (product **1**) along with a few colorless crystals of benzoic acid, which were removed by washing the product in a Buchner funnel with ethanol. The light-green crystalline product was dried in air. Yield of **1** based on the metal: 72 %. IR (UATR): $\tilde{\nu}$ = 3054 (vw), 2965 (br), 1593 (m), 1547 (s), 1494 (s), 1424 (s), 1384 (s), 1301 (m), 1070 (m), 1020 (m), 935 (m), 710 (s), 683 (s), 668 (s), 618 (s), 504 (s), 424 (m), 386 (m), 291 (s); 270 (s) cm^{-1}. $C_{14}H_{16}NiO_7$ (354.98): calcd. C 47.36, H 4.55; found C 46.85, H 4.68.

The magnetic properties of **1** were investigated using a commercial Quantum Design SQUID magnetometer in the temperature range 2–300 K at 0.1 T. A powder specimen of 62.130 mg was used. The data were corrected for the diamagnetic contribution with Pascal's constants using the MATRA program.[41]

Single-crystal X-ray data were collected at 295(2) K with an Oxford Diffraction Xcalibur diffractometer equipped with a Sapphire3 CCD detector and a graphite monochromator utilizing Mo-K_α radiation (λ = 0.71073 Å). The unit cell was chosen in accord with the recommendations of the International Union of Crystallography Commission on Crystallographic Data, using the shortest two axes in the (monoclinic) *ac* plane as unit-cell axes. In this case that gave a space group of *I*2/*a*.[42] Absorption corrections were based on the multi-scan technique and were performed using ABSPACK.[43] The structures were solved using SIR92[44] and refined against F^2 by full-matrix least-squares methods using SHELXL-2014/7.[45] Anisotropic displacement parameters were refined for all non-hydrogen atoms. The positional parameters of the hydrogen atoms bonded to the carbon and oxygen atoms were refined, with the isotropic displacement parameters assigned as 1.2U_{eq} of the corresponding bonding partners. The crystal and experimental data are given in Table 4, and selected geometric parameters are given in Table 1. Possible hydrogen bonds are presented in Table 2. The molecular crystal structures were drawn using Diamond.[46]

Table 4. Crystal data and structure refinement for **1**.

Empirical formula	$C_{14}H_{16}NiO_7$
M_r	354.98
Crystal system	monoclinic
Space group	*I*2/*a*
Unit cell dimensions	
a [Å]	6.1341(2)
b [Å]	34.1797(13)
c [Å]	6.9793(2)
β [°]	95.331(3)
V [Å^3]	1456.96(9)
Z	4
$D_{calcd.}$ [Mg/m^{-3}]	1.618
T [K]	295(2)
μ [mm^{-1}]	1.364
Crystal dimensions [mm]	0.16 × 0.04 × 0.02
Crystal color/form	light green, needle-like
Index ranges	$-7 \le h \le 7$
	$-43 \le k \le 44$
	$-9 \le l \le 9$
θ range [°]	4.182–27.474
Reflections collected	6276
Independent reflections	1638 (R_{int} = 0.0391)
Absorption corr. method	multi-scan
T_{min} – T_{max}	0.8438–1.0000
Goodness-of-fit on F^2	1.118
R indices [$I > 2\sigma(I)$]	*R*1 = 0.0433, wR_2 = 0.0936
R indices (all data)	*R*1 = 0.0582, wR_2 = 0.0996

CCDC 1408434 (for **1**) contains the supplementary crystallographic data for this paper. These data can be obtained free of charge from The Cambridge Crystallographic Data Centre.

Acknowledgments

This work was supported by the Slovak Grant Agencies (VEGA 1/0075/13, APVV-14-0078, and APVV-14-0073) and a European Regional Development Fund of the European Union (ERDF EU) grant (contract no. ITMS26220120047). Funding from the Ministry of Science and Innovation (Spain) (grants MAT2011-27233-C02-01 and MAT2011-27233-C02-02), the Diputación General de Aragón and the European Union Regional Development Fund is gratefully acknowledged. A. V. thanks the National Scholarship Programme of the Slovak Republic for financial support of her study stay at the University of Zaragoza (Spain). Dr. Rocío González Álvarez prepared Figure 5.

Keywords: Nickel · Carboxylate ligands · X-ray diffraction · Magnetic properties · Thermal properties

[1] F. Ephraim, A. Pfister, *Helv. Chim. Acta* **1925**, *8*, 369.
[2] P. Pfeiffer, S. V. Müllenheim, *J. Prakt. Chem.* **1933**, *137*, 9.
[3] S. F. Pavkovic, *J. Inorg. Nucl. Chem.* **1971**, *33*, 1475.
[4] A. B. Siqueira, E. Y. Ionashiro, C. T. de Carvalho, G. Bannach, E. C. Rodrigues, M. Ionashiro, *Quim. Nova* **2007**, *30*, 318.
[5] C. Balarew, D. Stoilova, R. Krasteva, *Thermochim. Acta* **1985**, *92*, 719.
[6] J. H. Deng, Y. P. Yi, Z. X. Xiong, L. Yuan, G. Q. Mei, *Acta Crystallogr., Sect. E: Struct. Rep. Online* **2009**, *65*, m1484.
[7] N. Stok, S. Biswas, *Chem. Rev.* **2012**, *112*, 933.
[8] Y. Z. Zheng, Z. Zheng, X. M. Chen, *Coord. Chem. Rev.* **2014**, *258–259*, 1.
[9] M. E. Andersson, M. Högbom, A. Rinaldo-Matthis, W. Blodig, Y. Liang, B. O. Persson, B. M. Sjöberg, X. D. Su, P. Nordlund, *Biochemistry* **2004**, *43*, 7966.
[10] J. L. Boer, S. B. Mulrooney, R. P. Hausinger, *Arch. Biochem. Biophys.* **2014**, *544*, 142.
[11] F. Meyer, *Prog. Inorg. Chem.* **2009**, *56*, 487.
[12] B. H. Ye, I. D. Williams, X. Y. Li, *J. Inorg. Biochem.* **2002**, *92*, 128.
[13] A. Karmakar, K. Deka, R. J. Sarma, J. B. Baruah, *Inorg. Chem. Commun.* **2006**, *9*, 836.
[14] M. Yamashita, T. Ishii, H. Matsuzaka, *Coord. Chem. Rev.* **2000**, *198*, 347.
[15] M. Cortijo, S. Herrero, B. Jerez, R. Jimenez-Aparicio, J. Perles, J. L. Priego, J. Torroba, J. Tortajada, *ChemPlusChem*, **2014**, *79*, 951.
[16] M. Orendáč, A. Orendáčová, J. Černák, A. Feher, P. J. C. Signore, M. W. Meisel, S. Merah, M. Verdaguer, *Phys. Rev. B* **1995**, *52*, 3435.
[17] C. Rudowicz, *Phys. B* **2014**, *436*, 193.
[18] E. Aydiner, C. Akyuz, *Chin. Phys. Lett.* **2005**, *22*, 2382.
[19] S. A. Zvyagin, J. Wosnitza, C. D. Batista, M. Tsukamoto, N. Kawashima, J. Krzystek, V. S. Zapf, M. Jaime, N. F. Oliveira, A. Paduan-Filho, *Phys. Rev. Lett.* **2007**, *98*, 047205.
[20] C. R. Choudhury, S. K. Dey, S. Sen, B. Bag, S. Mitra, V. Gramlich, *Z. Naturforsch. B* **2002**, *57*, 1191.
[21] M. James, *J. Chem. Soc., Dalton Trans.* **1998**, 2757.
[22] Z. L. Lu, P. Gamez, H. Z. Kou, C. H. Fan, H. T. Zhang, G. X. Sun, *CrystEngComm* **2012**, *14*, 5035.
[23] J. Černák, J. Chomič, D. Baloghová, M. Dunaj-Jurčo, *Acta Crystallogr., Sect. C* **1988**, *44*, 1902.
[24] J. Paharová, J. Černák, R. Boča, Z. Žák, *Inorg. Chim. Acta* **2003**, *346*, 25.
[25] J. Černák, N. Farkašová, M. Tomás, V. Kavečanský, E. Čižmár, M. Orendáč, *J. Coord. Chem.* **2015**, *68*, 2788.
[26] K. Nakamoto, *Infrared and Raman Spectra of Inorganic and Coordination Compounds, Part B: Applications in Coordination, Organometallic and Bioinorganic Chemistry*, Wiley, New York, **1997**.
[27] J. J. Han, Y. F. Niu, J. Han, X. L. Zhao, *Polyhedron* **2013**, *55*, 249.
[28] W. Ferenc, B. Cristovao, B. Mazurek, J. Sarzynski, *Chem. Pap.* **2006**, *60*, 207.

[29] a) W. W. Kaeding, R. O. Lindblom, R. G. Temple, H. I. Mahon, *Ind. Eng. Chem. Process Des. Dev.* **1965**, *4*, 97; b) J. Fraga-Dubreuil, J. Garcia-Serna, E. Garcia-Verdugo, L. M. Dudd, G. R. Aird, W. B. Thomas, M. Poliakoff, *J. Supercrit. Fluids* **2006**, *39*, 220.
[30] W. Buijs, *J. Mol. Catal. A* **1999**, *146*, 237.
[31] L. G. Qiu, L. N. Gu, G. Hu, L. D. Zjang, *J. Solid State Chem.* **2009**, *182*, 502.
[32] G. Novitchi, G. Pilet, D. Luneau, *Eur. J. Inorg. Chem.* **2011**, 4869.
[33] M. Fondo, N. Ocampo, A. M. Garcia-Deibe, J. Cano, J. Sanmartin, *Dalton Trans.* **2010**, *39*, 10888.
[34] S. S. Y. Chui, K. H. Low, J. Lu, V. A. L. Roy, S. L. F. Chan, C. M. Che, *Chem. Asian J.* **2010**, *5*, 2062.
[35] N. Masciocchi, G. A. Ardizzoia, S. Brenna, G. LaMonica, A. Maspero, S. Galli, A. Sironi, *Inorg. Chem.* **2002**, *41*, 6080.
[36] a) R. L. Harlow, S. H. Simonsen, *Acta Crystallogr., Sect. B* **1977**, *33*, 3234; b) M. M. Turnbull, *Acta Crystallogr., Sect. E* **2007**, *63*, m2148.
[37] H. Koizumi, K. Osaki, T. Watanabe, *J. Phys. Soc. Jpn.* **1963**, *18*, 117.
[38] R. Ivaníková, R. Boča, L. Dlháň, H. Fuess, A. Mašlejová, V. Mrázová, I. Svoboda, J. Titiš, *Polyhedron* **2006**, *25*, 3261.
[39] J. Chen, S. H. Wang, Z. F. Liu, M. F. Wu, Y. Xiao, R. Li, F. K. Zheng, G. C. Guo, *Inorg. Chem. Commun.* **2014**, *46*, 207.
[40] C. F. Macrae, P. R. Edgington, P. McCabe, E. Pidcock, G. P. Shields, R. Taylor, M. Towler, J. van de Streek, *J. Appl. Crystallogr.* **2006**, *39*, 453.
[41] J. Marek, Z. Trávníček, *Program MaTra for Magnetic Calculations*, Palacký University in Olomouc, Czech Republic, **2001**.
[42] O. Kennard, J. C. Speakman, J. D. H. Donnay, *Acta Crystallogr.* **1967**, *22*, 445.
[43] R. H. Blessing, *Acta Crystallogr., Sect. B* **1995**, *51*, 816; R. H. Blessing, *J. Appl. Crystallogr.* **1997**, *30*, 421.
[44] A. Altomare, G. Cascarano, C. Giacovazzo, A. Gualardi, *J. Appl. Crystallogr.* **1993**, *26*, 343.
[45] G. M. Sheldrick, *Acta Crystallogr., Sect. C* **2015**, *71*, 3.
[46] K. Brandenburg, H. Putz, *Crystal Impact Diamond*, Crystal and Molecular Structure Visualization, Bonn, **2008**.

Received: October 31, 2015
Published Online: January 15, 2016